THE PHYSICS OF ANALYTICAL FERROGRAPHY

By

KARUNAKARAN S. NAIR

Bachelor of Science

University of Kerala

Trivandrum, India

1970

Submitted to the Faculty of the Graduate College
of the Oklahoma State University
in partial fulfillment of the requirements
MASTER OF SCIENCE
December, 1980

THE PHYSICS OF ANALYTICAL FERROGRAPHY

Thesis Approved:

Thesis Adviser

Dean of Graduate College

PREFACE

This study is concerned with the development of basic equations which govern the process of particle deposition on an Analytical Ferrogram. The primary objective is to determine the reasons for the data scatter and the difficulty in calibration of the Ferrographic process. Based on the derived equations for particle deposition, a mathematical model to predict the area covered by the particles at any location on the slide is presented.

The author wishes to express his appreciation to his major adviser, Dr. E. C. Fitch, for his guidance and assistance throughout this study and his Master's program. The opportunity given to the author at the Fluid Power Research Center by Dr. Fitch in improving his knowledge in the area of fluid power is well appreciated. Appreciation is also expressed to other committee members, Dr. R. L. Lowery and Dr. J. Murali, for their interest in this area of study and help given to the author.

A note of thanks is given to Dr. R. K. Tessmann and Mrs. J. D. Dobson for the opportunity to learn about Ferrography. Thanks are also extended to Ms. Diana McAngus for typing the thesis in spite of her busy schedule.

Finally, special gratitude is expressed to my parents and to my friend, Mr. K. N. B. Panicker, for their encouragement throughout my studies.

TABLE OF CONTENTS

LIST OF FIGURES

NOMENCLATURE

A	constant of Ferrogram
b	width of the Ferrogram deposit
C	constant of integration
D	diameter of wear particles
dx_o	region from where particles deposit at dz_p
dz_p	region where area covered is evaluated
F_d	force on the particles due to viscous drag
F_g	force on the particles due to gravity and buoyancy
F_m	force induced on the particles due to magnetic induction
g	acceleration due to gravity
H	field of the magnet on the Ferrograph
i	subscript to denote a specific size of particles
K	magnetic volume susceptibility of the wear particles
k	subscript to denoting particle size
m	a constant to describe the variation of magnetic parameters along the slide
n	number of particles
P_i	total number of particles of diameter D_i
Q	volume flow rate of fluid over the slide
R_e	flow Reynolds number over the slide
r	subscript to denote size of particles
S	total area covered by particles in the region dz_p

S_i	area covered by particles of diameter D_i in the region dz_p
U_z	velocity of fluid over the slide in z-direction
$U_z(max)$	maximum value of U_z
$U_z(ave)$	average value of U_z
V_T	settling velocity
V_x	velocity of particle in x-direction
V_z	velocity of particle in z-direction
w	width of U-boundary on slide
X	x-axis direction
x	x-coordinate at any point with respect to coordinate axis
x_o	initial location of particle in the fluid as it enters the slide
x_p	x-coordinate of the particle
Z	z-axis direction
z_p	location of deposition of particles on the slide
$z_p(max)$	maximum possible z_p for a given particle
β	inclination of slide to vertical
δ	fluid film thickness over the slide
ρ_f	density of fluid
ρ_p	density of particle
μ	viscosity of fluid

CHAPTER I

INTRODUCTION

Monitoring lubricating and hydraulic fluids for wear particles has been accepted as a realistic and economic method for diagnosis and prediction of machine malfunctioning. It has long been recognized that when wear in a machine increases, the number and size of particles generated at the interface between the moving parts also increase. These wear particles are swept away by the oil passing through the wearing surfaces. By monitoring the fluid for the number and size of the particles, the state of the machine can be predicted.

Most of the wearing surfaces are made of iron and hence are magnetic. If the size and number of iron particles in the fluid increase, it can be expected that the machine is undergoing a serious wear mode. Based on this concept the Foxboro Analytical Group developed a machine called Ferrography to separate wear particles from a fluid sample by means of a powerful permanant magnet (1) (2). Among different configurations of the Ferrographs available, the Analytical Ferrograph is the most promising one because the particles can be observed under a microscope.

From a number of experiments at the Fluid Power Research Center and other laboratories, it has been observed that there exists a substantial amount of scatter in the data obtained from the machine. A large number of controlled experiments conducted at the Fluid Power Research Center

could not identify the reasons why this scatter is occurring. Since these experiments failed to give clues for this scatter, it was necessary to approach the problem analytically and see whether information could be obtained to explain the scatter in the data from the Ferrograph. This could lead to a better machine if the parameters affecting the Ferrographic process could be controlled.

This thesis presents the development of a mathematical model to express the trajectory of the particles in the sample fluid when subjected to gravity, viscous and magnetic forces. It is assumed for convenience that the wear particles are spherical in nature. The effect of shape, concentration and number of particles on the mathematical equations is discussed qualitatively in the thesis.

CHAPTER II

PREVIOUS INVESTIGATION

Magnetic separation of ferrous particles has been utilized for years for benefication of ores. Ferrography was the first equipment of its kind which could separate small wear particles and then facilitate an in depth analysis of the particles by optical methods. Essentially the Ferrograph is an experimental innovation. Many users of the machine conducted numerous experiments to formulate a standardized procedure (3) (4) (5) (6), so that the consistency in data and particle deposition could be obtained, irrespective of the machine or laboratory.

Kitzmiller (7) attempted to develop an analytical model for the Ferrograph, but due to the complexity of the parameters involved in the physics of the machine, he limited his work to an experimental evaluation. He was unable to predict the reason for scatter of particle deposition based on his experiments.

Because of the problems involved in the standardization of the Ferrographic process, four laboratories in U.S.A. joined together in a round robin project to experimentally develop a standardized procedure for Ferrographic operation (8). This was expected to give enough consistency of the Ferrographic data. To date no success was achieved from such an effort. Presently, plans are being made for another round robin project. Recently, the Society of Automotive Engineers formed a committee to look into the standardization of the Ferrographic process

(9). This work is only in the initial stages.

The bibliography included in this thesis presents a number of literature citations on Ferrography. Thus far, no experiments have been proposed which could identify the the behavior of the particles in the fluid sample. Further, no analytical model has ever been successful. Accordingly, this thesis is expected to fill this vacuum. Hopefully, this model will uncover the problem and lead to a modification of the machine so that performance of the machine can be improved.

CHAPTER III

MODEL OF THE FERROGRAPH

Figure 1 shows a schematic of the Analytical Ferrograph. The fluid sample contained in a sample bottle is pumped through a capillary tube by a peristaltic pump onto a glass slide. The fluid flows down the slide under the force of gravity to a drain tube. A high gradient (large force) magnet positioned below the slide captures the magnetic particles onto the slide while the non-magnetic particles tend to be washed away by the fluid.

Ideal Ferrograph

To study the trajectory and deposition of the particles, it is convenient to conceive an idealized Ferrograph which operates under certain assumed conditions. Any deviation from this idealized situation can be studied by the variation of the Ferrographic process by each of the specific parameter. Thus the following assumptions are made for modeling the Ferrograph:

1. The particles - of wear and non-wear origin - are uniformly distributed in the sample.

2. The peristaltic pump delivery is uniform when flow reaches the slide.

3. The flow of fluid across the slide is uniform one dimensional type laminar flow.

4. The laminar flow over the slide has a low Reynolds number so that the flow is ripple free. Appendix B gives supporting calculations to show this assumption is correct.

5. There is no initial disturbance in the flow as the fluid enters the slide, since Reynolds number is low.

6. Fluid properties are unaffected by the presence of particles in the sample since particle concentration is low.

7. Brownian forces do not act on the particles and the motion of the particles can be idealized based on the fundamental laws of fluid mechanics and magnetic phenomena.

8. The wear particles are spherical in nature.

Except for the last assumption, all other are quite valid. The assumption of spherical particles renders easy analysis. This is true only for fatigue wear particles in certain cases (10).

The change of shape of the particles will be considered as a deviation from the idealized condition and accordingly a discussion is presented to include these effects.

Flow Over the Slide

The slide over which the sample fluid flows is made of rectangular thin glass sheet of about 60 millimetres in length. Oil enters the slide at about 55.5 to 56.6 millimetres from the exit end where fluid leaves the slide. The gravity flow over the slide is contained in a U-shaped boundary. Figure 2 is a schematic of the slide where wear particles are shown to have been deposited.

The sample fluid flows as a partially developed rivulet on the slide. Flow of the fluid is controlled by the inclination of the slide

to vertical, surface tension, fluid viscosity, and the density of the sample fluid. Towell and Rothfeld (11) have developed the hydrodynamics of a fully developed rivulet flow as a one-dimensional laminar flow. A closed form flow model is necessary for studying particle dynamics in the fluid. Using the theory they developed for the purpose of modeling the flow over the slide suffers from two disadvantages: firstly, it requires numerical techniques denying a closed-form solution; and secondly, on the Ferrogram, the flow is not allowed to expand laterally on the slide due to the presence of the U-boundary on the slide. Since there is no full bounding wall on either side of the flow stream as in the case of a channel, and since the width of the flow film is not large, the flow is not exactly the "open channel" type. Thus, the flow tends to be somewhere in between open channel flow and a fully developed rivulet flow. Figure 3 shows the difference between the cross-section of the fluid film under these conditions. On the Ferrogram, however, the major interest is in the central region of the fluid flow, where the ferrous particles are deposited. Ferrous particles in the fluid are attracted towards the center of the slide due to the existence of lateral field gradient of the magnet. Thus, the central region reasonably represents open channel flow.

Figure 4 shows the coordinatres selected for analyzing the fluid flow. In this diagram, the positive X-direction is measured vertically upwards from the slide, where fluid contacts the substrate. The Y-direction is measured in a lateral direction from the center line, while the Z-direction is measured along the flow from the point of entry of the fluid on the slide.

With the assumption of open-channel flow, the velocity profile of

the fluid flow over the slide is parabolic. This velocity in the Z-direction can be represented by (12) (13):

$$U_z = \frac{\rho_f g \cos\beta}{2\mu}(2\delta x - x^2) \tag{1}$$

where U_z = the fluid velocity along the flow direction, ρ_f = the density of the fluid, β = the inclination of the slide to the vertical, μ = the viscosity of the fluid, x = the height of the streamline above the slide where velocity is evaluated, and δ = the maximum height of the flowing film. The velocity profile is shown in Figure 5.

The maximum value of velocity, as shown by Equation (1), is at the interface between the air and the sample fluid and this is obtained by substituting $x = \delta$ in Equation (1). Maximum velocity, $U_z(max)$, is given by:

$$U_z(max) = \frac{\rho_f g \delta^2 \cos\beta}{2\mu} \tag{2}$$

Volume rate of flow over the slide is given by:

$$Q = \frac{\rho_f g w \delta^3 \cos\beta}{3\mu} \tag{3}$$

where Q = the volume rate of flow of fluid over the slide, and w = the width of the U-boundary on the slide.

Again, the average velocity of the fluid flow, $U_z(ave)$, on the slide is given by:

$$U_z(ave) = \frac{\rho_f g \delta^2 \cos\beta}{3\mu} \tag{4}$$

Equation (1) through Equation (4) show the general nature of the flow over the slide.

Particle Dynamics

When the fluid flows over the slide, the particles suspended in them will be subjected to gravity, buoyant force, drag force, and magnetic forces. In the flow direction, i.e. the z-axis, the particles will be carried by the fluid. Since the flow velocity is very low, the forward velocity of the particle will be approximately the same as the fluid velocity. Accordingly, Equation (1) represents the particle velocity, if fluid velocity U_z, is replaced by the particle velocity, V_z. Hence,

$$V_z = \frac{\rho_f g \cos\beta}{2\mu}(2\delta x_p - x_p^2) \tag{5}$$

Equation (5) gives the velocity of the particles in the z-direction. Another equation in the x-direction as described below will completely define the motion of the particle.

Figure 5 shows the forces acting on any particle in the x-direction.

The net force on any particle due to gravity and buoyancy which is acting downward can be represented as:

$$F_g = \frac{g\pi D^3}{6}(\rho_p - \rho_f) \tag{6}$$

where F_g = the net downward force due to gravity and buoyancy, D = the diameter of the particle, and ρ_p = the density of the particle.

Since the Reynolds number is low, the drag force in the vertical direction can be represented by Stoke's Law as given below:

$$F_d = 3\pi\mu D V_x \tag{7}$$

where F_d = the drag force in the x-direction, and V_x = the velocity of the particle in the x-direction.

In addition to the above forces, the magnetic particles are subjected to an additional force due to the presence of the high gradient magnet below the slide. This can be represented by (1) (14):

$$F_m = \frac{\pi D^3}{6} \text{ K.H. } \frac{dH}{dx} \tag{8}$$

where F_m = the magnetic force in the x-direction, K = the volume susceptibility of the material, H = the field strength of the magnet at the point of interest, and dH/dx = the field gradient which is constant across the fluid film height.

Equation (6), (7) and (8) can be combined to give the net force acting on the particle in the x-direction. The particle is accelerated by the net force acting in the x-direction. By Newton's law:

$$F_g - F_d + F_m = \frac{\pi D^3}{6} \rho_p \cdot \left(\frac{dV_x}{dt}\right) \tag{9}$$

where dV_x/dt = the acceleration of the particle in the x-direction.

Substituting Equations (6), (7) and (8) into Equation (9):

$$\frac{\pi D^3}{6}\left[g(\rho_p - \rho_f) + KH \frac{dH}{dx}\right] - 3\pi\mu D V_x = \frac{\pi D^3}{6} \rho_p \cdot \left(\frac{dV_x}{dt}\right) \tag{10}$$

The particle acceleration in the fluid according to Equation (10), until the gravity and magnetic forces balance the drag force. At this stage, the particle reaches its settling velocity (V_T). Hereafter, the particle travels with uniform velocity (V_T) in the x-direction. The settling velocity can be computed by setting the right-hand side of Equation (10) equivalent to zero, and replacing V_x by V_T. Settling velocity (V_T) can, then be represented as:

$$V_T = \frac{D^2}{18\mu}\left[g(\rho_p - \rho_f) + KH \cdot \frac{dH}{dx}\right] \tag{11}$$

Combining Equations (10) and (11),

$$V_T - V_x = \frac{D^2 \rho_p}{18\mu} \left(\frac{dV_x}{dt}\right) \tag{12}$$

Equation (12) is a linear, first-order, differential equation in V_x, and its solution is:

$$V_x = V_T \left[1 - \exp.\ (-18\mu/D^2\rho_p)\ t\right] \tag{13}$$

From Equation (13), the time required for particle velocity to reach 98% of the settling velocity (V_T) can be evaluated as $(4D^2\rho_p/18\mu)$.

It is convenient to check how much time is necessary for a particle to reach its settling velocity. As a highly conservation approach, consider a steel particle of diameter 20 micrometres in a thin fluid such as water whose viscosity is about 1 centipoise. Assuming the density of steel as 8 grams per cubic centimetre, this time will be:

$$\frac{4(20 \times 10^{-4}\text{cm})^2(8\text{gm/cm}^3)}{18(0.01\ \text{gm/cm-sec})} \cong 7 \times 10^{-4}\text{seconds}$$

Thus, the particle velocity reaches 98% of its settling velocity in a fraction of a second; and hence, it can be assumed that the particle dynamics in the x-direction, that is, along the depth of the film thickness, is controlled by the settling velocity. If x_p is the position of the particle from the slide at any time, then,

$$\frac{dx_p}{dt} = -V_T \tag{14}$$

The negative sign for V_T is introduced as per the sign convention, since V_T acts in the negative x-direction. Equation (5) and (14) define the dynamics of the magnetic particles in the flowing fluid. They can be combined by eliminating the variable time (t). Dividing Equation (5)

by Equation (14) and rearranging;

$$dz_p = \frac{-\rho_f g\cos\beta}{2\mu}(2\delta x_p - x_p^2)\frac{dx_p}{V_T} \tag{15}$$

Integrating Equation (15) yields:

$$z_p = -\frac{\rho_f g\cos\beta}{2\mu V_T}(\delta x_p^2 - x_p^3/3) + C \tag{16}$$

where C = the constant of integration.

The particle may enter at any height above the slide in the fluid film. Denoting this height as x_o (See Figure 4), the initial condition in the above equation would be: $x_p = x_o$ at $z_p = 0$.

Setting this initial condition, in the above equation, yields:

$$C = \frac{\rho_f g\cos\beta}{2\mu V_T}(\delta x_o^2 - x_o^3/3) \tag{17}$$

The position of a given particle when it is deposited on the Ferrogram slide is the position z_p when x_p is forced to zero. Substituting $x_p = 0$ in Equation (16) gives:

$$z_p = C = \frac{\rho_f g\cos\beta}{2\mu V_T}(\delta x_o^2 - x_o^3/3) \tag{18}$$

Substituting the value of V_T from Equation (11) and that of δ from Equation (2) into Equation (18) yields:

$$z_p = \frac{9\rho_f g\cos\beta\left[(3\mu Q/\rho_f g w\cos\beta)^{1/3}x_o^2 - x_o^3/3\right]}{D^2\left[g(\rho_p - \rho_f) + KH\frac{dH}{dx}\right]} \tag{19}$$

Equation (19) defines the location of a particle on the Ferrogram, if x_o and D are known. However, this equation is derived assuming that the magnetic term, KH (dH/dx) remains constant along the length of the Ferrogram. The high gradient, dH/dx, varying along the length of the Ferrogram. Accordingly, Equation (19) should be modified to take care

of the variation of magnetic properties.

In the Ferrogram, it is observed that large size particles (particles whose sizes are larger than 15μm in diameter) are deposited within 5 millimetres from the entry point. If representative values are substituted for various parameters in Equation's (16) and (17), the relative values of the gravity term, $g(\rho_p - \rho_f)$ and the magnetic term, KH (dH/dx) can be evaluated such that a particle of 15μm gets deposited within 5 millimetres from entry point. Typical values of the parameters are:

fluid density, $\rho_f = 0.8$ gm/cc

particle density, $\rho_p = 8$ gm/cc

acceleration due to gravity, $g = 980$ cm/sec^2

inclination of slide with respect to horizontal, $\beta \cong 88.5°$

film thickness, $\delta = (3\mu Q/\rho_f g\cos\beta)^{1/3} = 0.1$ cm (assume)

particle diameter, $D = 15 \times 10^{-4}$ cm

position of particle deposition, $z_p = 0.5$ cm

Further, assume that the particle enters the slide at the maximum film height location, that is, $x_o = \delta$. With these parameters substituted into Equation (19), and solving for KH (dH/dx), KH (dH/dx) = 1.25×10^5 dynes/cc. The value of $g(\rho_p - \rho_f)$ would be $g(\rho_p - \rho_f) = 0.07 \times 10^5$ dynes/cc. Thus from this illustration, it can be concluded that the contribution of the magnetic forces in the Ferrographic process is much stronger than that from the gravity term.

Based on the results of the foregoing analysis, the settling velocity, V_T, in Equation (11) can now be represented as containing only the magnetic term, that is,

$$V_T = \frac{D^2 \, KH \, \frac{dH}{dx}}{18\mu} \tag{20}$$

It is seen from Equation (20) that the effect of increasing H (dH/dx) along the Ferrogram slide is to directly increase the settling velocity. But if Equation (20) is modified to this effect, then the variation of H (dH/dx) and, hence settling velocity, V_T, should be known. To evaluate the magnitude of H (dH/dx) or its variation over a small region of the magnet is extremely difficult, if not impossible. Even experimental measurements may not give these values to an acceptable accuracy because of the short range of effective magnetic field and smaller force magnitudes on micronic particles (14) (15) (16) (17) (18) (19). The trend of the variation of (dH/dx) along the slide is indicated by Miller (20) as a polynomial function of x. The variation of H, dH/dx, and H (dH/dx) are shown in Figure 6. The product H (dH/dx) is approximated to be an exponential function H $(dH/dx)e^{mz}$ along the z-direction (m is a constant). Subsequently, the settling velocity at various locations on the slide, that is, as z_p varies, will have an exponential variation. This can be represented as:

$$V_s = V_T e^{mz} \tag{21}$$

where V_s = the settling velocity of the particle as a function of its location along the Ferrogram; V_T = the settling velocity of the particle as given by Equation (20); m = a constant; and z = the distance along the z-direction, where V_x is required to be evaluated. (Note that the magnetic term, KH (dH/dx), in Equation (20) represents its value only at or near the entry location.)

Now, the motion of the particle along the depth of fluid film,

that is, x-direction, as given by Equation (14) must be modified to take care of the change in settling velocity along the Ferrogram. This can be expressed as:

$$\frac{dx_p}{dt} = V_s = -V_T(\text{exp. } mz) \tag{22}$$

Now Equations (5) and (22) represent the complete dynamics of the particles anywhere along the length of the fluid film. Dividing Equation (5) by Equation (22) and rearranging, yields:

$$e^{mz_p} dz_p = -\frac{\rho_f g \cos\beta}{2\mu V_T} (2\delta x_p - x_p^2)\, dx_p \tag{23}$$

Integrating this equation between the entry point and the point where the particle gets deposited on the slide (that is, x_p, from x_o, to 0; z_p, from 0 to z_p), produces,

$$\frac{1}{m}(e^{mz_p} - 1) = \frac{\rho_f g \cos\beta}{2\mu V_T} (2\delta x_p - x_p^3/3) \tag{24}$$

From this equation, the location of the particle, z_p, is

$$z_p = \frac{1}{m} \ln\left\{1 + m \cdot \frac{\rho_f g \cos\beta}{2\mu V_T} (\delta x_p^2 - x_p^3/3)\right\} \tag{25}$$

Equation (25) is similar to Equation (18) except that it includes the effect of the variation of magnetic properties along the length of the slide. Note that z_p in the above equation is the location of a magnetic particle on the slide in an idealized situation, presented in the beginning of the paper.

The purpose of the derivation of the above equation was solely to demonstrate the effect of the variation of magnetic forces on particle deposition rather than absolute evaluation. Equation (25) clearly

indicates that the effect of increasing the magnetic gradient along the exit end of the Ferrogram is to deposit the larger size particles as close as possible to the entry location. It is seen that the effect of various parameters like x_o, μ, Q, etc., are masked by the equation because of the logarithmic function; however, this need not be true in general. This is because, firstly, in the case of bigger particles, Equation (18) gives the correct picture of z_p since they are deposited near the entry. Secondly, smaller particles get saturated magnetically as they have only one or at best few magnetic domains (2) (14). Accordingly, Equation (18) should be valid for any magnetic particle in the sample fluid. Hence, it could be stated that the effect of variation in the magnetic properties, H (dH/dx), of particles is to confine larger size magnetic particles to the upper region of the Ferrogram.

CHAPTER IV

ANALYSIS OF THE EQUATIONS

The information obtained from the Ferrogram slide are both quantitative as well as qualitative. Quantitative wear analysis is the evaluation of wear debris based on the amount and size of wear debris. Qualitative wear analysis is a subjective evaluation of the size and material of the particles and the types of wear mode by observation under a microscope. The qualitative analysis does not depend on the location of the particles on the slide. Whereas, the quantitative analysis is an objective evaluation where the amount of particles deposited on a given location on the slide is significant.

Because of the difficulty in measuring small amount of wear debris, the quantity of wear particles at any location is obtained by measuring the amount of light blocked by the particles on the slide over a one millimetre diameter aperture. This procedure, of course, assumes that not more than one layer of particles is present at any location. An attempt is made here to obtain a closed form solution to represent the area covered by wear particles deposited on the slide.

Let there be n_1 particles of diameter D_1, n_2 particles of diameter D_2, etc. in the oil sample volume so that total number of particles in the fluid, n, is:

$$n = \sum_{i=1}^{k} n_i \tag{26}$$

where k is the total number of different particle sizes in the fluid.

Assume that the sample contains only ferrous particles. Again, consider a given fluid so that viscosity and flow rate are constant. Now, Equation (19), can be represented as:

$$z_p = \frac{9\rho_f g\delta^3 \cos\beta \left[\left(\frac{x_{oi}}{\delta}\right)^2 - \frac{1}{3}\left(\frac{x_{oi}}{\delta}\right)^3 \right]}{D_i^2 \left[g(\rho_p - \rho_f) + KH \frac{dH}{dx} \right]} \tag{27}$$

$$= \frac{A}{D_i^2} \left[\left(\frac{x_o}{\delta}\right)^2 - \frac{1}{3}\left(\frac{x_o}{\delta}\right)^3 \right] \tag{28}$$

where

$$A = \frac{9\rho_f g\delta^3 \cos\beta}{g(\rho_p - \rho_f) + KH \frac{dH}{dx}} \tag{29}$$

A is the constant of the Analytical Ferrogram for a given fluid and material of the particle. When a particle starts at the top of the fluid film i.e. at $x_o = \delta$, the particle reaches the maximum deposit location, i.e. $z_p = z_p(\max)$. Substituting $x_{oi} = \delta$ in Equation (28)

$$z_p(\max) = \frac{2}{3} \frac{A}{D_i^2} \tag{30}$$

In other words, a given location on the slide, consists of different size particles starting from a size D_r to D_k. This situation is clearly depicted in Figure 7. Particles larger than D_r deposit upstream of this location.

Consider any location, z_p, on the slide. (Figure 8) To evaluate the deposition of particles in this location, a certain region of length, dz_p, is taken around the location, z_p. In this region dz_p, particles of different sizes are deposited as per Equation (28). For example, take the case of particles of diameter D_1 reaching at a height

x_{01} (see Figure 9). Particles of diameter D_1 reaching in a certain height range dx_{oi} travels in a trajectory to deposit in the location dz_p. Similarly, particles of any diameter D_r travel from a region dx_{or} deposit in the same region as dz_p. The total number of particles of any given diameter D_i deposited at dz_p can be statistically represented as:

$$P_i = \left(\frac{dx_{oi}}{\delta}\right) n_i \tag{31}$$

where P_i is the total number of particles of diameter D_i, which are deposited at dz_p. This statistical assumption of equal probability for particles to reach any film height is quite valid because of the large number of wear particles.

The area, S_i, covered by these particles of diameter D_i, is:

$$S_i = P_i\left(\frac{\pi D_i^2}{4}\right) \tag{32}$$

Substituting Equation (31) into Equation (32), yeilds

$$S_i = \frac{dx_{oi}}{\delta} n_i \left(\frac{\pi D_i^2}{4}\right) \tag{33}$$

Total area, S, covered by all the particles in the region dz_p is contributed from particles of sizes D_r to D_n.

$$S = \sum_{i=r}^{k} \frac{dx_{oi}}{\delta} n_i \left(\frac{\pi D_i^2}{4}\right) \tag{34}$$

Equation (34) represented the total area covered by all the particles at region dz_p. This equation is meaningful only if the parameter dx_{oi} is eliminated. dx_{oi} from Equation (34) can be eliminated by the following process.

1. Select a given location z_p where the area covered is to be

evaluated.

2. Using the selected z_p, solve the cubic Equation (28) for x_{oi}.

3. Differentiate Equation (28) to obtain dz_p and dx_{oi}. In this equation, substitute x_{oi} from the previous step.

4. Solve for dx_{oi} and then substitute this value in Equation (34).

Clearly this process does not lead to a closed form solution because of the cubic and quadratic equations involved. Fortunately, the whole process of eliminating dx_{oi} in Equation (34) can be simplified as follows:

Figure 10 shows a graph to represent Equation (28). It is seen that this graph shows a straight line relationship between x_o/δ and $z_p D_i^2/A$, such that

$$z_p = \frac{A}{D_i^2}\left(\frac{x_{oi}}{\delta} - 0.25\right), \quad \frac{x_o}{\delta} \quad 0.25 \tag{35}$$

The most important region for analysis on the slide is the first eight millimetres from the entry point. This is because the wear particles above two micrometres deposit in this region. The entry point is discarded for analysis because there is a pile of wear particles in that region (5). The reason for this piling is quite evident from Figure 10, because 25 percentage of particles is deposited in the first 10 percent of maximum possible particle travel. Accordingly, if for severe wear particles of 20μm size, the maximum distance possible is three millimetre according to Equation (30), then 25 percent of all these particles of 20μm deposit within the first 0.3 millimetre, i.e. the entry point.

Equation (35) can be alternately written as:

$$x_{oi} = \delta \left[\frac{D_i^2}{A} z_p + 0.25 \right] \tag{36}$$

Now x_{oi} is available and hence the total area covered at any location can be obtained using Equation (34).

Differentiating Equation (36),

$$dx_{oi} = \frac{\delta D_i^2}{A} dz_p \tag{37}$$

Combining Equation's (34) and (37)

$$S = \sum_{i=r}^{k} \frac{\pi}{4A} D_i^4 n_i dz_p \tag{38}$$

Referring to Figure 8. This area, S represents the area of particles in a rectangular strip of dimensions b and dz_p. If dz_p is set as the diameter of aperture of the densitometer, then the area by the particles, S_o can be represented as:

$$S_o = \frac{\pi}{4} \frac{S}{b} \tag{39}$$

Substituting Equation (38) into Equation (39)

$$S_o = \frac{\pi^2}{16Ab} \sum_{i=r}^{k} D_i^4 n_i dz_p \tag{40}$$

Equation (40) shows that the area covered is the fourth power of diameter. This shows the power of Ferrograph in grading particles predominance according to size along the Ferrogram. Hence by measuring the area covered at different locations, the severity of wear mode can be assessed.

CHAPTER V

VARIATION FROM IDEAL PROCESS

Effect of Particle Shape

The equations presented in the thesis were derived based on the assumption that the particles are spherical in nature. Normally only fatigue wear particles from roller bearings are seen to be spherical. Wear particles from cutting wear, rubbing wear, etc., are found to be platelets, flakes, propeller shaped or sometimes slender particles. Plate like particles if they move downward on their edges, the drag force will be 3 to 4 times smaller than if their plane is parallel to slide. The general trend of these platelets is to fall on edges because of the influence of magnet. Subsequently they fall near entry location.

Propeller shaped or curly particles develop lift forces on them and rotate in the fluid as they travel (21). Hence they may travel farther distance than if they were spherical particles. However, the high gradient magnetic field should confine the particles not to travel farther from the entry point as was shown by Equation (25). Moreover, the magnetic field causes particles to align with the field so that they are forced to travel in unison. The only exception possible to this situation is highly slender and curly particles which disobey Stoke's law due to lift forces. These particles can deposit disobeying

the magnetic field.

Since there are so many types of shapes of particles that are possible, generalization is not possible. However, based on the discussion presented here, the model presented for spherical particles appears to apply for other shaped particles as well.

Effect of Sample Volume and Concentration

The model presented is independent of the sample volume of fluid and concentration of wear particles. The large sample volume should only increase the time of operation of the machine. However, a large concentration of particles cause the particles to agglomerate and subsequently affect the distribution of the particles over the slide.

CHAPTER VI

DISCUSSION ON THE MODEL

The motivation for development of the model in this thesis was the scatter of data from experiments conducted by various laboratories. The following difficulties were observed in conducting an experiment which could be used to validate the model.

1. Absence of a method to measure the magnetic field in the small distance of film height.

2. Unavailability of a contaminant whose size, distribution, density and magnetic properties are known.

3. Absence of flow visualization technique to observe the movement of micronic particles in the fluid film.

4. Deformation of plastic tube used in the peristaltic pump causing slow flow variation. This necessitates a modification of the pumping mechanism.

5. Occasionally the plastic tube used was found to trap wear particles in the area where pump rollers were applying pressure. This caused problems for precise assessments of wear debris.

Rectification of the problems cited above is beyond the scope of the present work. Based on the model developed, a discussion is advanced in this chapter for obtaining an overall view of the deposition of the particles on the slide.

Equation (19) in Chapter III defines the location of the deposition of any particle onto the slide. From this equation, it is seen that there are a number of variables which can affect the Ferrographic process. The parameters which affect the process are discussed in the following pages. When applicable, representative numerical values have been used for a more clear understanding. Appendix C gives the details of the numerical values used.

Consider a case when the properties of sample fluid and the wear particles are known. In such case the only parameter unknown in Equation (19) is x_o, the initial height of the particles as they enter the slide. The value of x_o is uncontrollable and hence deposition of a given particle is not predictable as per Equation (19). Figure 10 shows this effect of x_o on particle deposition. Also, it is seen from Figure 10 that lower the value of x_o, the deposition becomes very nearer to the entry point. On page 20 of the thesis, it was mentioned that the nonlinear behavior in Figure 10 causes piling of particles at entry point.

The dependence of the particle deposition on x_o is such that any location on the slide can have particles of various sizes. This situation was schematically shown in Figures 7 and 9. However, according to Equation (30) and as shown in Figure 7, particles of a given size and material can travel only a certain maximum distance, z_p (max). The magnitude of z_p (max) depends on the diameter of the particles. Figure 11 shows how z_p (max) varies as a function of particle diameter. Figure 11 is drawn based on Equation (30) and appropriate numerical values from Appendix C.

Since fluids used for analysis using Ferrography have different viscosity, it may be worthwhile to see the effect of viscosity on the model. It is seen from Equation (19) that the viscosity and flow rate appear as a product μQ in the model. The flow through the pipe through which the fluid sample flows to the slide is laminar: and hence the flow should be inversely proportional to the viscosity of the fluid. In other words, the product μQ should be constant. Accordingly the particle deposition is independent of the change in flow rate due to variations in viscosity of the fluid.

Ferrography is based on the magnetic property of wear particles; however, there are non-magnetic as well as weakly magnetic particles in the sample which may be from extraneous sources. The effect of material of the particle on deposition on the slide can be explained as follows:

Magnetic property of the wear particles appear in the model as K, the volume susceptibility of the material of the particle. Higher the value of K, the stronger the force applied by the magnet on the particle. Consider particles of 10 micrometers diameter of different materials. Keeping K as a variable, substitute representative numerical values from Appendix C into Equation (27). For various values of (x_o/δ), a family of curves can be obtained to demonstrate the effect of K on particle deposition, as shown in Figure 12.

From Figure 12, when particles start at top of fluid film, i.e. $(x_o/\delta) = 1.0$, the particles are washed away to drain bottle, if K is less than 110. Particles made of aluminum, brass, stainless steel, etc. have their values of K less than 110. However, when $(x_o/\delta) = 0.25$ even these non-magnetic or weakly magnetic particles are deposited on

the slide, as seen from Figure 12.

The diameter of the particles was assumed to be 10 micrometers for drawing the graph in Figure 12. Particles larger than 10 micrometer will be deposited nearer to the entry and vice versa as per Equation (27) and Figure 11.

Figure 12 brought out the influence of x_o, the initial location of particles as they enter the slide, on particle deposition. Implicitely, Figure 12 suggests that if particles are injected into the fluid near the top of the fluid film, then the deposition of particles is predictable. In such a case when x_o is controlled non-magnetic particles will be washed away to drain bottle.

CHAPTER VII

CONCLUSIONS

Conclusions derived from this study may be stated as follows:

1. The physics of the Analytical Ferrograph was studied and presented the governing equations needed to describe the particle deposition on the slide presented.

2. Parameters affecting the Ferrographic process were identified. Of these the initial position of the particle as it enters the slide, x_o, was found to be most critical.

3. The reason for the presence of small particles near the entry region was presented. This in contrary to the concept that the Ferrograph will grade the particles according to size, through this is experimentally and now analytically not true.

4. The increasing magnetic field towards the exit end of the slide does not affect the particle deposition as long as large particles (greater than say 5μm) are concerned.

5. Even though small particles are also deposited near the entry region, the area covered is unaffected by them. This is because the area covered is a function of the fourth power of the diameter of the particles.

6. If a method can be devised to inject particles at a given height, x_o, into the film, the statistical nature of the Ferrograph in terms of deposition of particles can be annulled.

7. The effect of the shape of particles was qualitatively discussed in the thesis.

8. Finally, the model revealed the reasons for the scatter of data from the machine which was observed by many experimentalists and users of the machine.

Recommendation for Further Study

1. Previous efforts to standardize the Ferrographic process failed due to the scatter in data. Since a new round robin project and an SAE Committee have been formed for the purpose, this model will help provide a new look for this standardization process. Accordingly the standardization procedure should aim at:

   a. Selecting standard contaminant of known size and prepare artifical fluid samples.

   b. Observe area covered by wear particles at maximum number of locations possible.

   c. Repeat the experiments with actual wear particles ensuring that non-wear particles are pre-separated before running the slide.

2. Investigate the possibility of studying the movement of particles in the fluid. Fibre optic borescopes can probably be used for this purpose.

3. Investigate the possibility of replacing the peristaltic pump by a pneumatic pressurizing system so that slow flow variations can be annulled.

4. Since the area covered is a function of the fourth power of the diameter, it may be possible that by knowing the area covered over

a few points, the severity of the wear can be quantitatively found by processing this information.

5. By controlled experiments and by knowing the particle deposition, the magnetic parameter H dH/dx can be evaluated on the Ferrogram. Knowledge of H dH/dx will be helpful to know whether the magnetic parameters remain the same for different machines.

6. Configurations other than plane slide, such as channel shape, will provide a controlled flow over the slide. It is recommended that studies should be conducted for alternate configurations of the slide. Such studies can consider increasing the flow rate over the slide so that time for running a sample can be reduced.

A SELECTED BIBLIOGRAPHY

1. Seifert, W. W., and Westcott, V. C. "A Method for the Study of Wear Particles in Lubricating Oil," Wear, Vol. 21 (1972), pp. 27-42.

2. Westcott, V. C. Method and Apparatus for Segregating Particulate Matter, U.S. Letters, Patent No. 4,047,814, Issued on September 13, 1977.

3. Ruff, A. W. Study of Initial Stages of Wear by Electron Channeling - Part 2: Quantitative Methods on Wear Debris Analysis, Institute of Material Research, National Bureau of Standards, Report No. NBSIR 76-1141, September, 1976.

4. Sample Preparation/Ferrogram Procedure/Ferrogram Analysis, Tribology Laboratory, Naval Air Engineering Center, Lakehurst, New Jersey, September 7, 1978.

5. Tessmann, R. K. "Non-Intrusive Analysis of Contaminant Wear in Gear Pumps through Ferrography." (Unpublished Ph.D. thesis, Mechanical Engineering Department, Oklahoma State University, Stillwater, Oklahoma, 1977.)

6. Hofman, M. V., and Johnson, J. H. The Development and Application of Ferrography to the Study of Diesel Engine Wear, Society of Automotive Engineers, Paper No. 70181. Presented at the Congress and Exposition, Detroit, Michigan, February-March, 1978.

7. Kitzmiller, D. E. "The Development of a Calibration Technique and Standard Operating Procedures for a Ferrograph." (M.S. thesis, Oklahoma State University, Stillwater, Oklahoma, 1977.)

8. "Round Robin Ferrography Verification Program." (Unpublished Report, Naval Air Engineering Center, Lakehurst, New Jersey, 1978.)

9. Ferrography Task Force Number SAE-ORMTC, SC-4. (Unpublished Correspondence, Society of Automotive Engineers, Fluid Power Research Center, Oklahoma State University, Stillwater, Oklahoma, September, 1980.)

10. Bowen, E. R., and Westcott, V. C. Wear Particle Atlas. Burlington, Massachusetts: Foxboro/Trans/Sonics Inc., 1976.

11. Towell, G. D., and Rothfeld, L. B. "Hydrodynamics of Rivulet Flow." A.I.Ch.E Journal, Vol. 12 (1962), No. 5, pp. 972-980.

12. Bird, R. W., Stewart, W. E., and Lighfoot, E. N. Transport Pehnomena. New York: John Wiley & Sons, 1960.

13. Giles, R. V. Fluid Mechanics and Hydraulics. New York: Schaum Publishing Co., 1962.

14. Bozorth, R. M. Ferromagnetism. Princeton, New Jersey: Van Nostrand Inc., 1955.

15. Luborsky, F. E. "High Field--High Gradient Magnetic Separation: A Review," Proceedings of 21st Annual Conference on Magnetism and Magnetic Materials. Philadelphia, 1975.

16. Barrett, W. T., Lawver, J. E., and Wright, J. L. "Rapid Method of Evaluating Magnetic Separator Force Patterns." Transactions of the Society of Mining Engineers. AIME, Vol. 27 (September, 1973), pp. 231-232.

17. Watson, J. H. P. "Magnetic Filtration." Journal of Applied Physics. Vol. 44 (1973), No. 9, pp. 4209-4213.

18. Oberteufter, J. A. "High Gradient Magnetic Separation." Transactions on Magnetics, IEEE, Vol. MAG-9 (September, 1973), pp. 303-306.

19. Oberteufter, J. A. "Magnetic Separation: A Review of Principles, Devices, and Applications." Transactions on Magnetics, IEEE, Vol. MAG-10 (June, 1974), pp. 223-238.

20. Miller, R. S. "Discussion on Ferrography." Proceedings of the Workshop on Tribology, Atlanta, October, 1973.

21. Happel, J. and Brenner, H. Low Reynolds Number Hydrodynamics. Englewood Cliffs, New Jersey: Prentice-Hall Inc., 1965.

22. Kitzmi-ler, D. E. and Tessmann, R. K. "The Capabilities and Limitations of Ferrographic Wear Analysis." The BFPR Journal, Vol. 11 (1978), No. 1, pp. 87-94.

23. Parsons, D. A. "Speed of Sand Grains in Laminar Flow Over a Smooth Bed." Fort Collins, Colorado: Proceedings on Sedimentation, Colorado State University (1972), Chapter I.

24. Taggart, A. F. Handbook of Mineral Dressing. New York: John Willey & Sons, Inc., 1945.

25. Reda, A. A., Bowen, R., and Westcott, V. C. "Characteristics of Particles Generated at the Interface Between Sliding Steel Surfaces." Wear, Vol. 34 (1975), pp. 261-273.

26. Anderson, D. P. Ferrographic Analysis for Hydraulic Fluids. SAE Paper No. 790873, October, 1979.

27. Nair, K. S. "An Appraisal of the Direct Reading (DR) Ferrograph." The BFPR Journal, Vol. 13 (1980), No. 4, pp. 319-328.

28. Nair, K. S. "An Appraisal of the Analytical Ferrographic Method." The BFPR Journal, Vol. 3 (1980), No. 3, pp. 281-294.

29. Nair, K. S. "The Effect of Non-Magnetic and Weakly Magnetic Particles on the Ferrographic Proces." The BFPR Journal, Vol. 14 (1981), No. 2, pp. 155-161.

30. Dobson, J. D. and Nair, K. S. "Some Observations on the Efficiency of Ferrographic Process." (Unpublished FPRC Report, 1980.)

31. Bittle, R. R., and Nair, K. S. "The Applications of Ferrography for Fire Resistant Fluids." (Unpublished FPRC Report, 1980.)

APPENDIX A

FIGURES

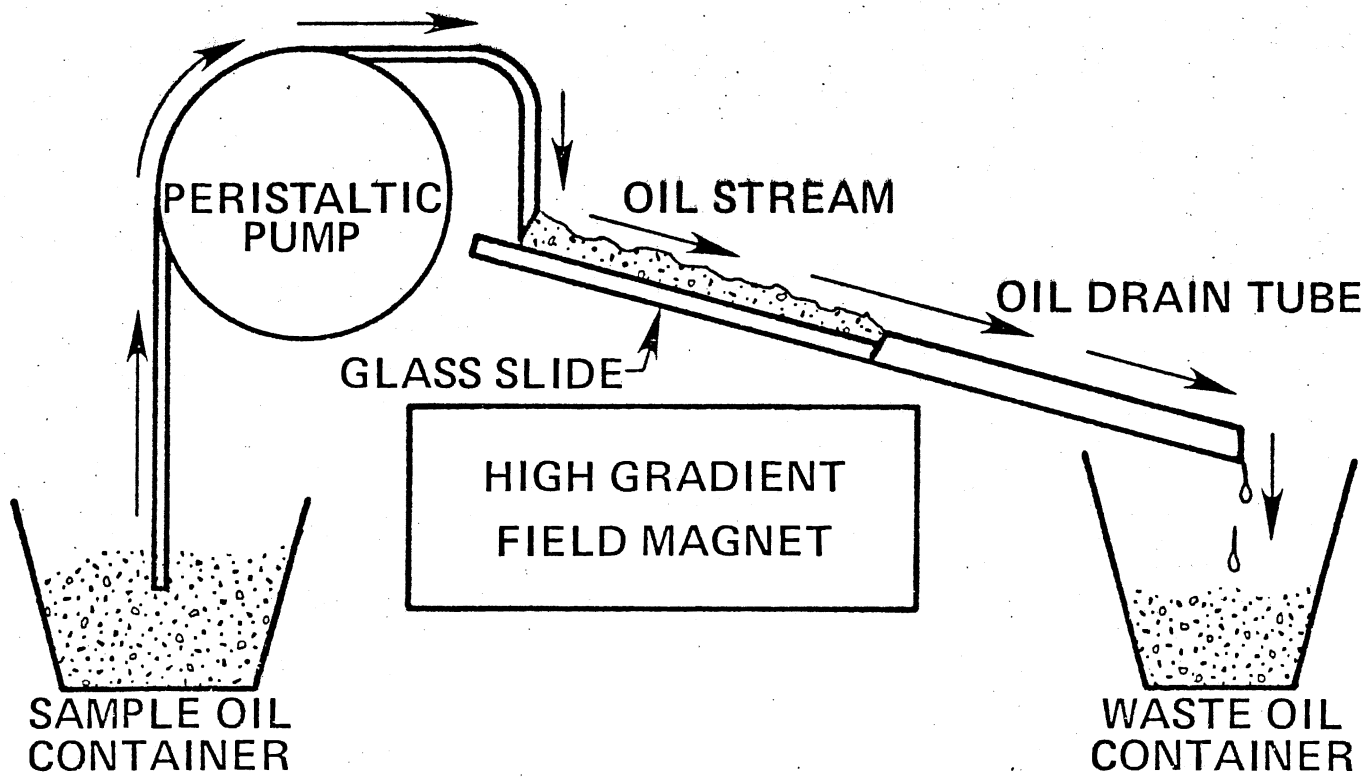

Figure 1. Schematic of an Analytical Ferrograph

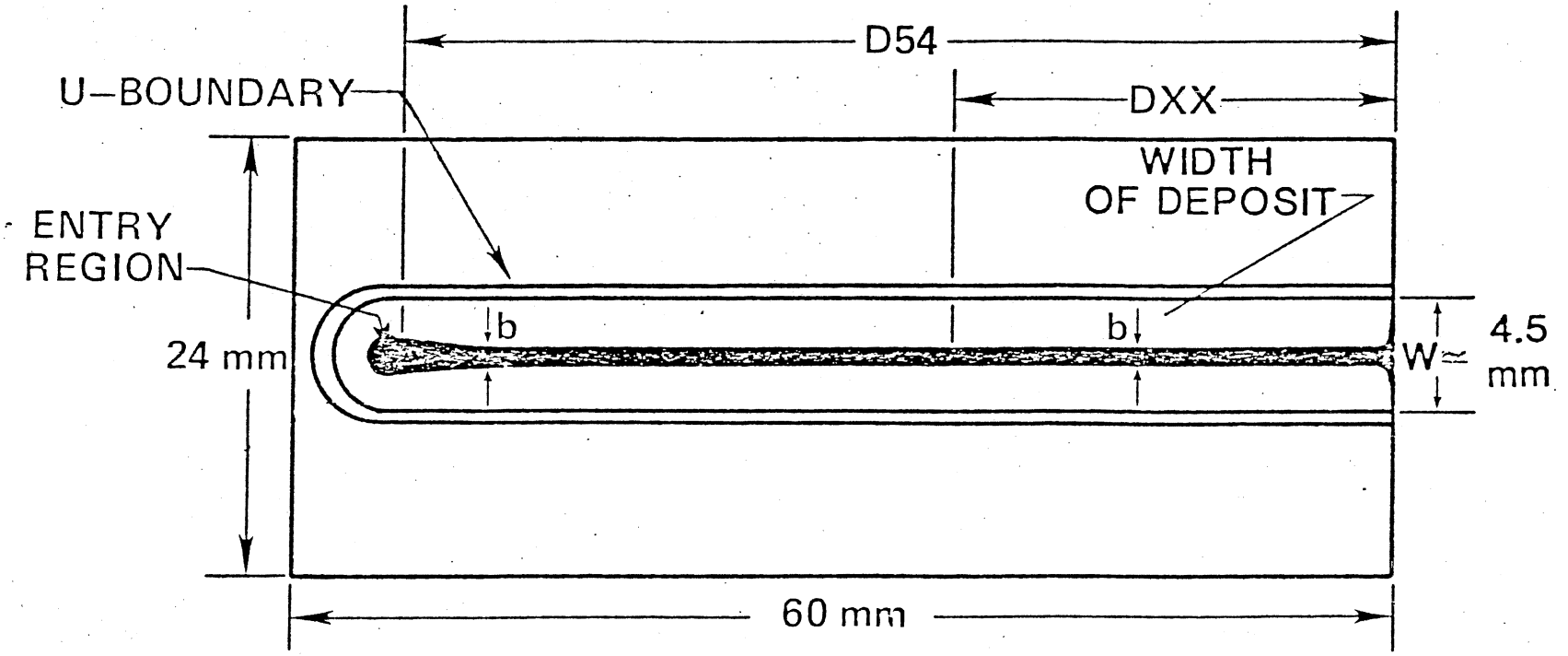

Figure 2. Major Dimensions of a Slide Including the Wear Deposit

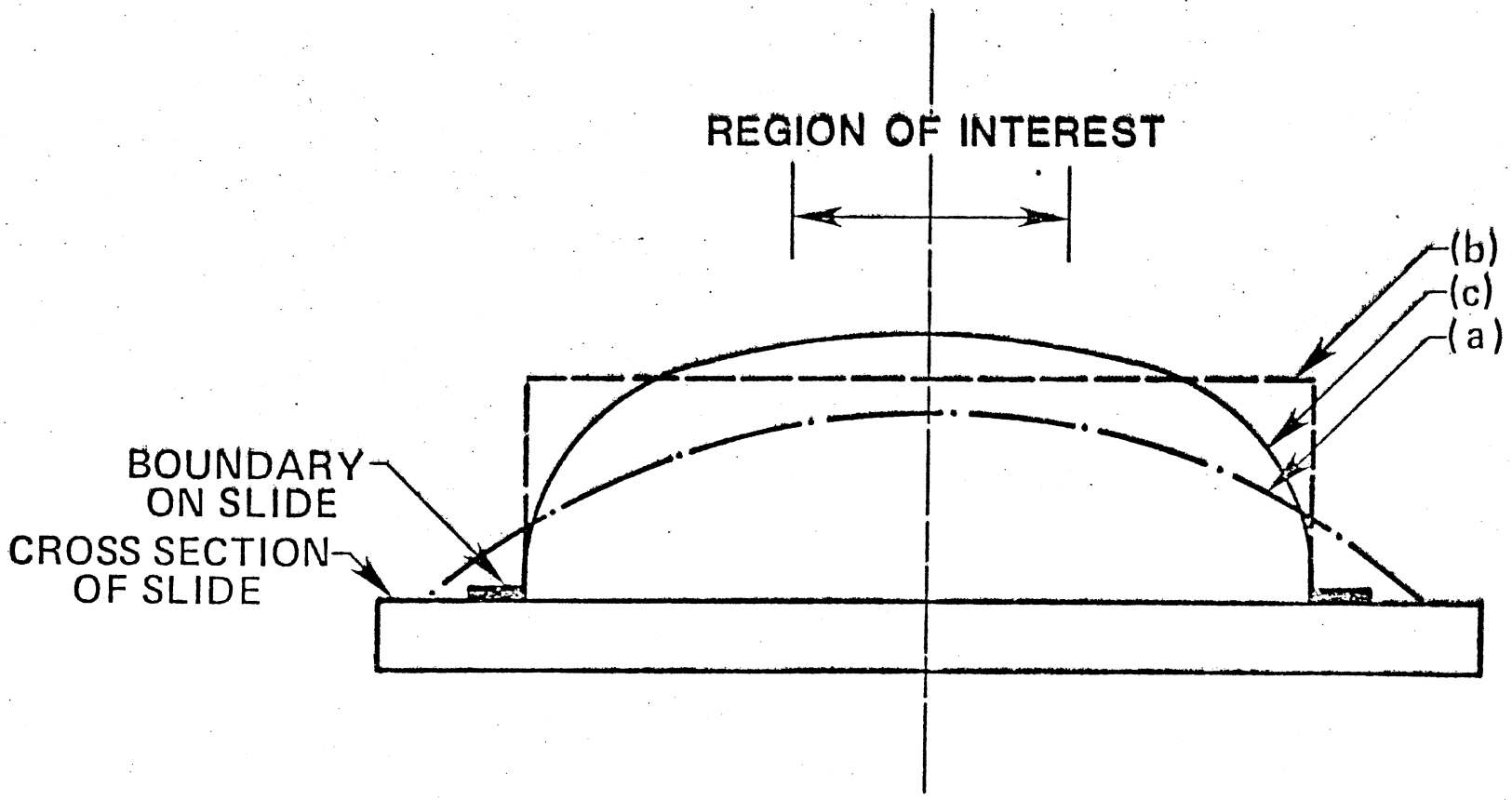

Figure 3. Cross Sections of Fluid Film Under Various Flow Boundaries
a) Fully Developed Rivulet Flow
b) Open Channel Flow
c) Flow Over Ferrogram Slide

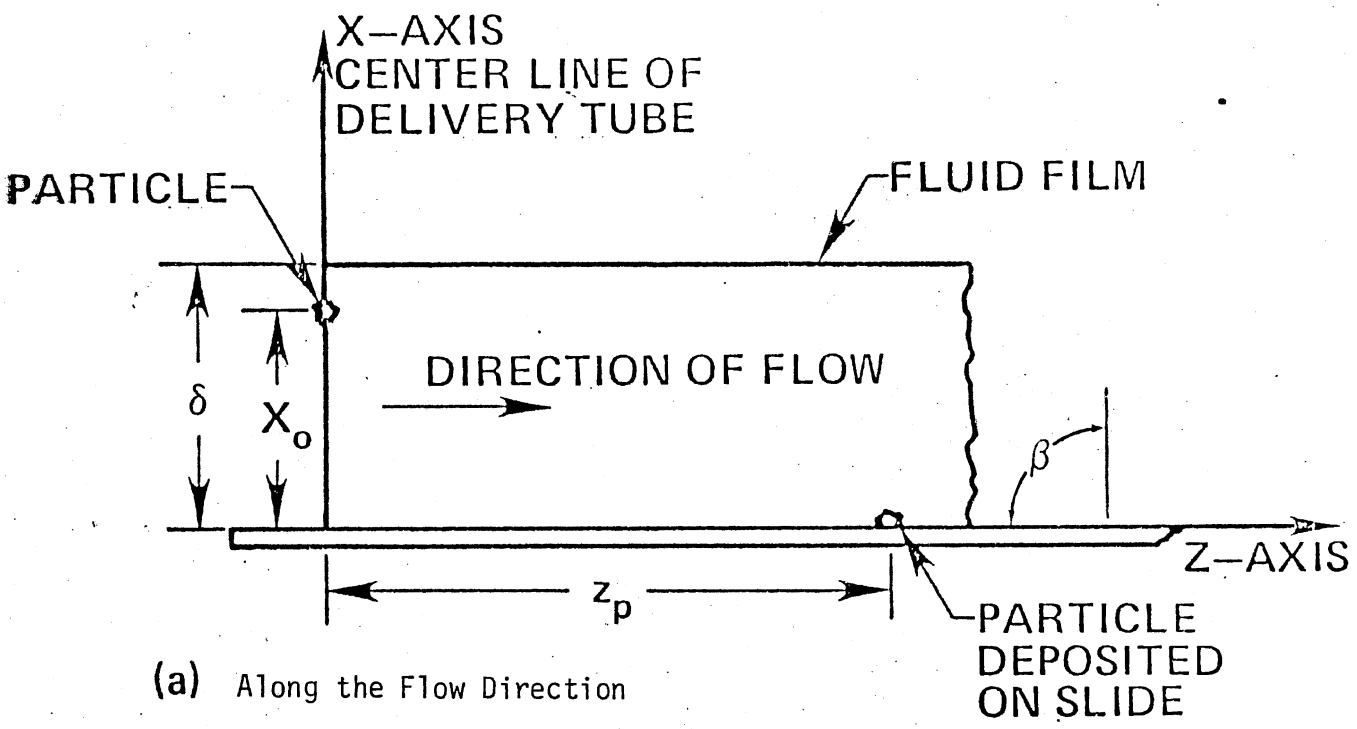

(a) Along the Flow Direction

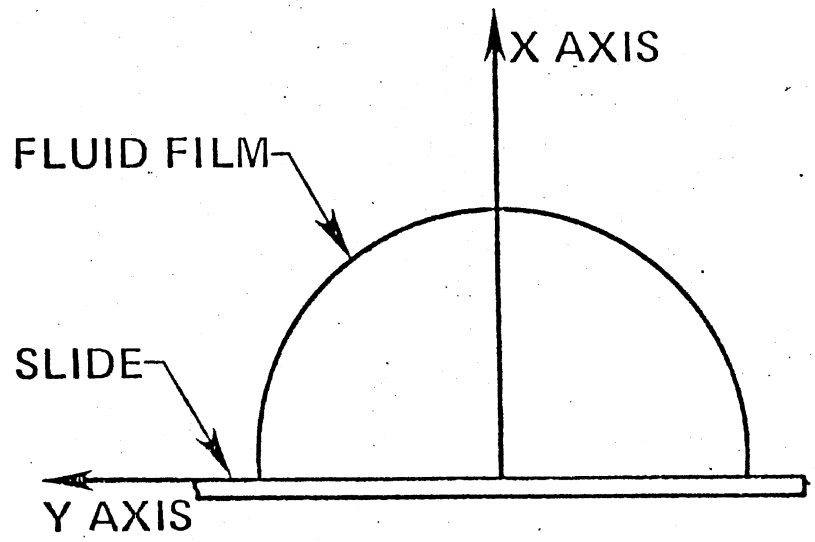

(b) Across the Section of Fluid Film

Figure 4. Co-ordinates Selected for the Model

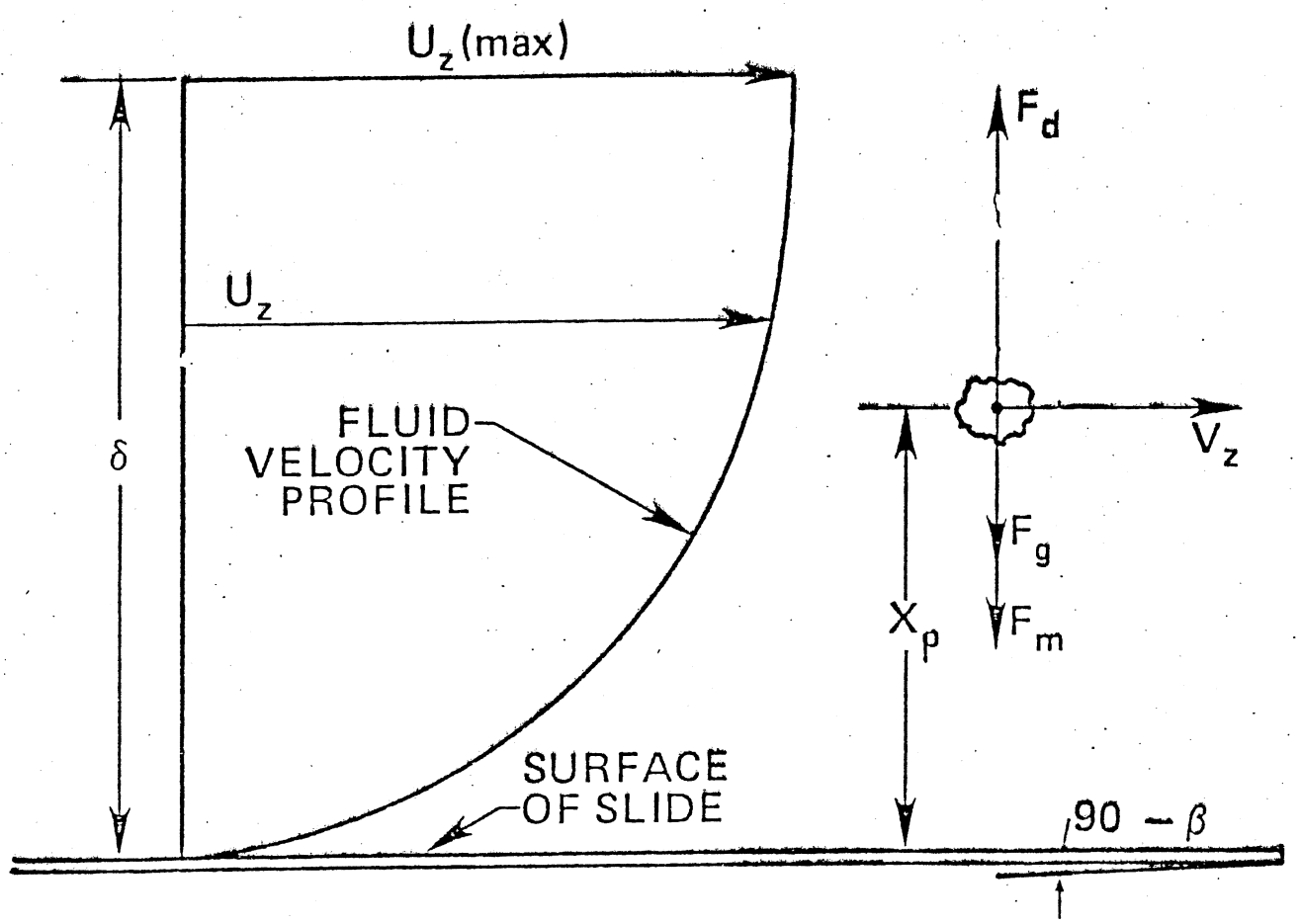

Figure 5. The Velocity Profile Over the Slide and the Forces on the Particles in X-direction

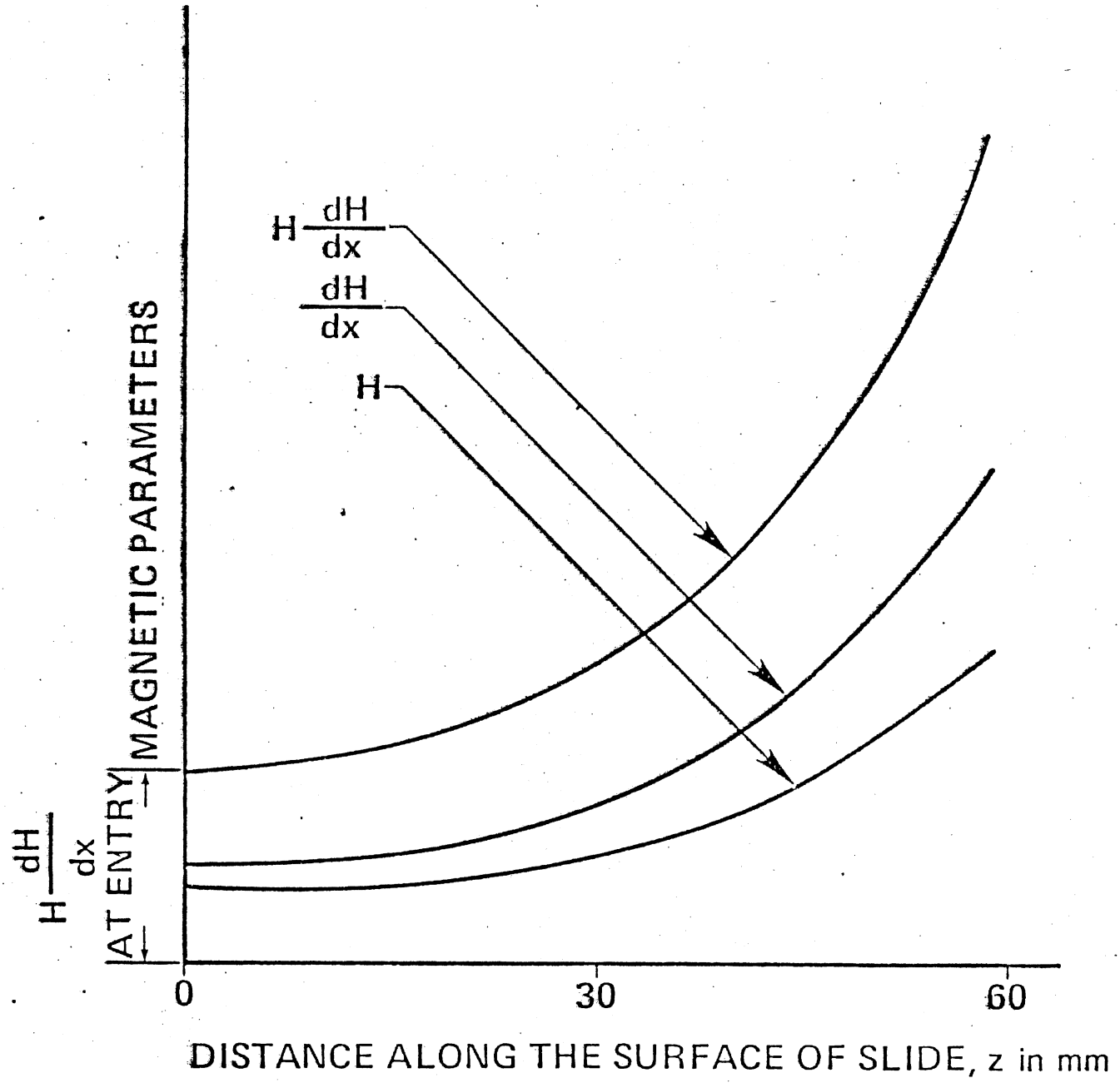

Figure 6. Variation of Magnetic Parameters Along the Slide

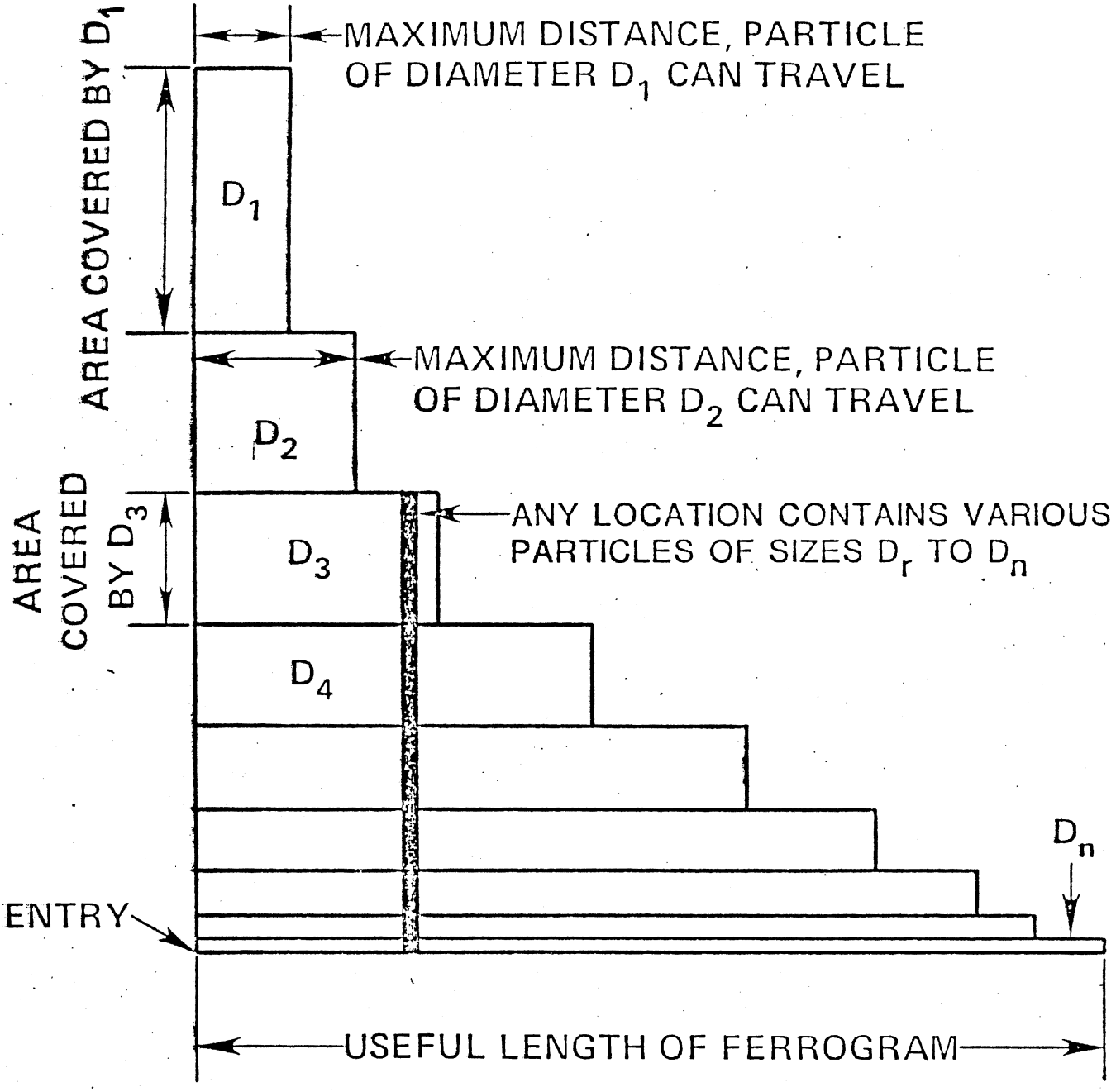

Figure 7. Range of Travel for any Given Size Particle

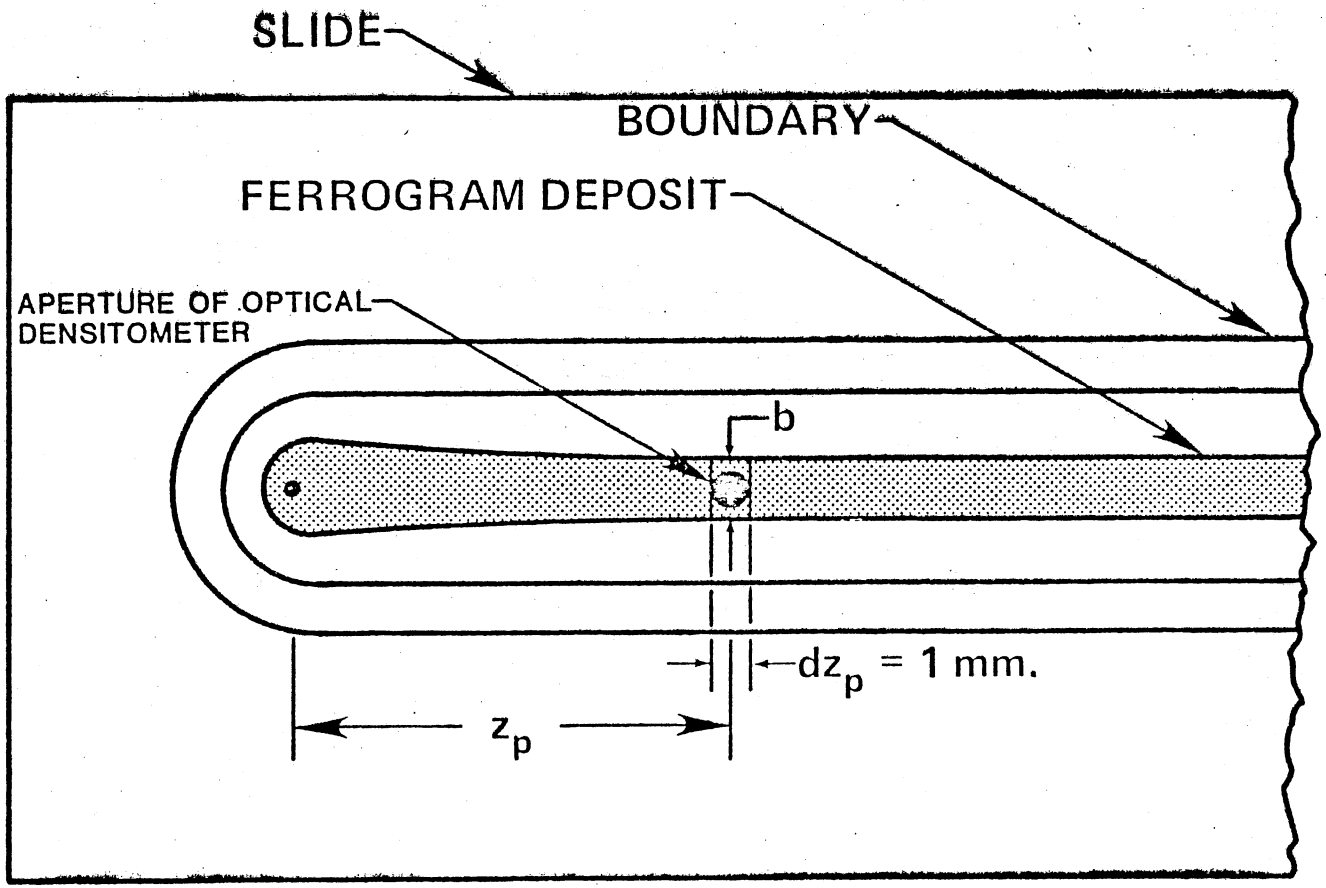

Figure 8. Aperture of the Optical Densitometer

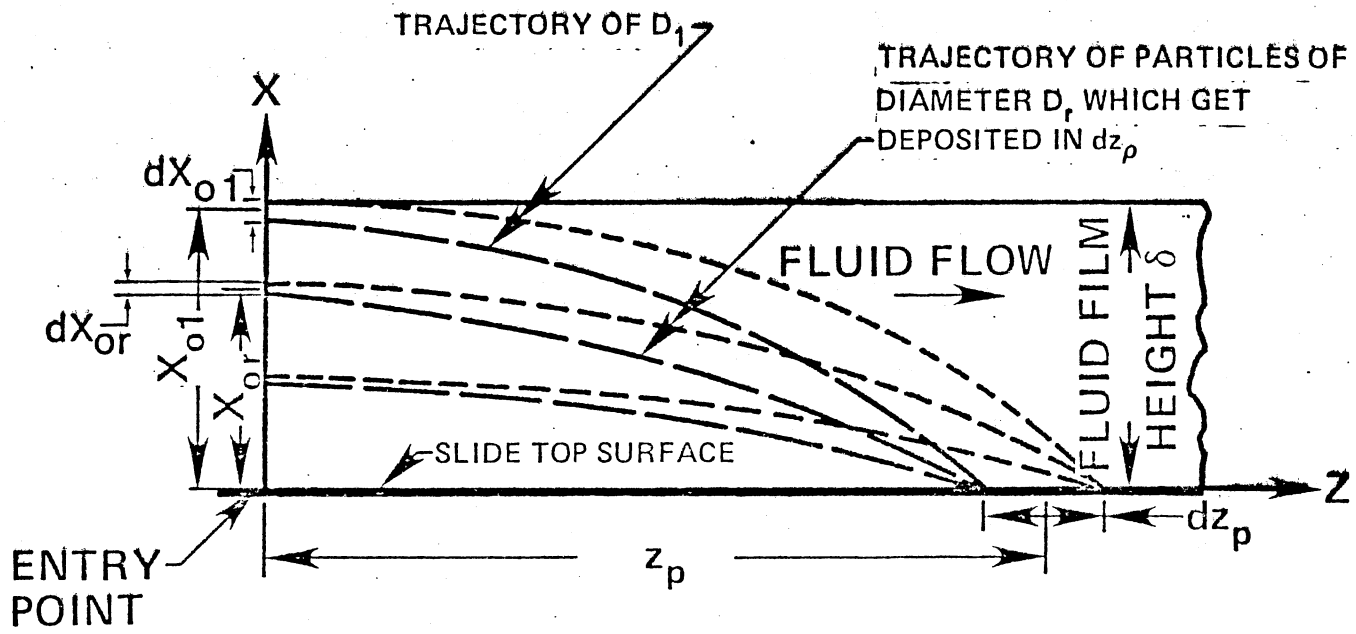

Figure 9. Trajectory of Particles as a Function of Initial Location and Diameter

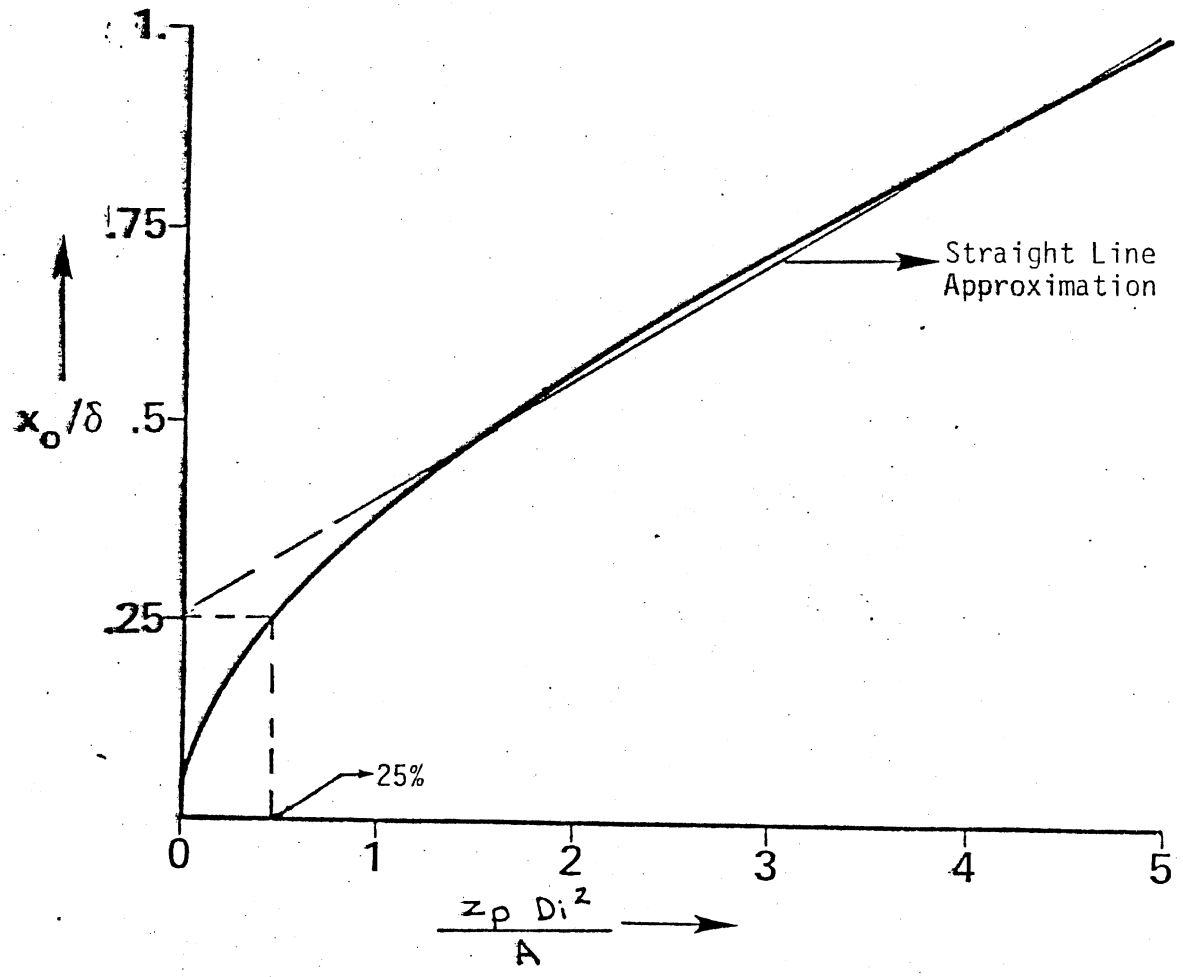

Figure 10. Plot of Equation 10 Showing Linear Approximation

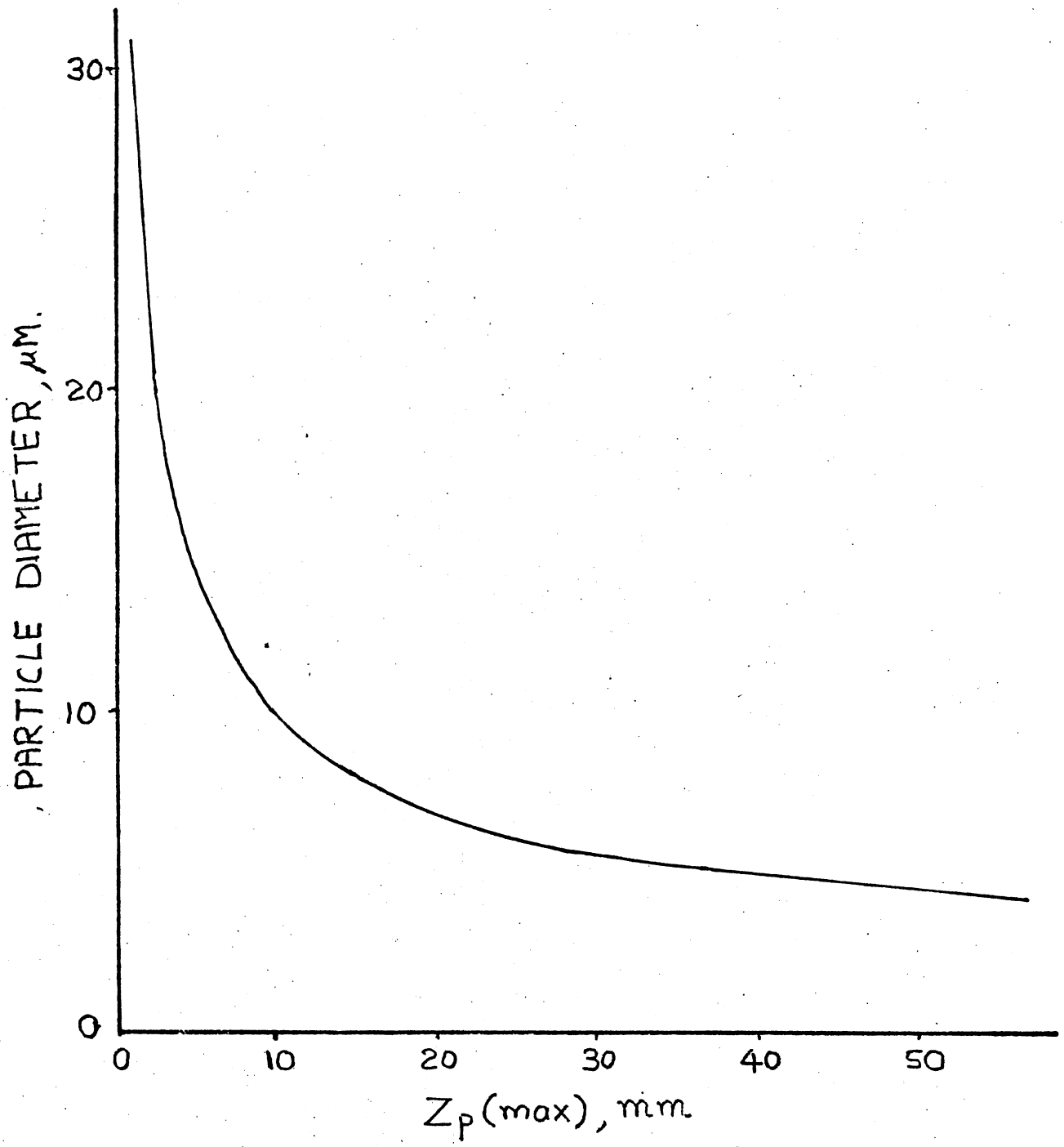

Figure 11. Variation of Maximum Possible Particle Travel With Respect to Particle Diameter

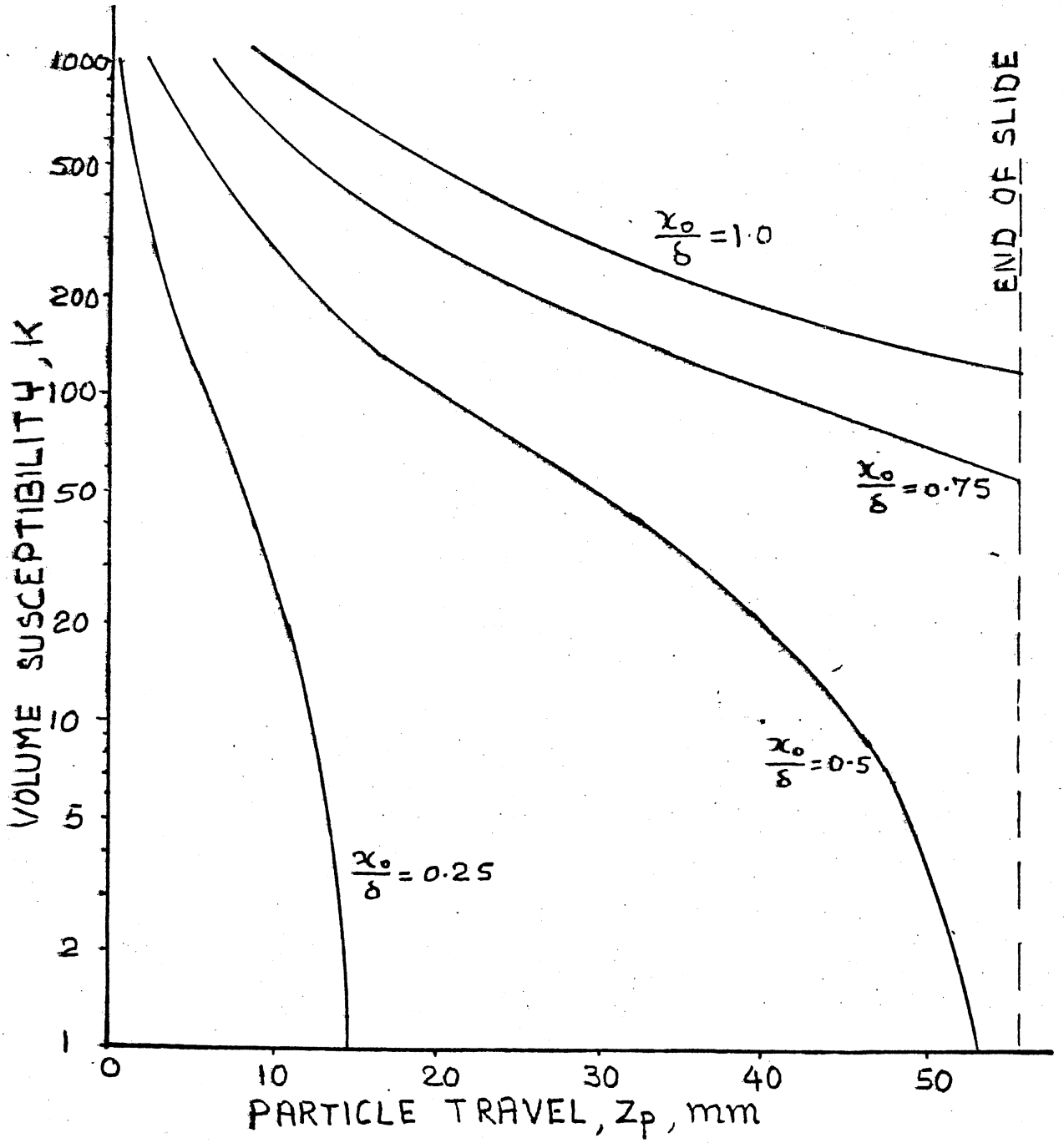

Figure 12. Effect of Magnetic Property of Material on Deposition of a 10 μm Particle

APPENDIX B

FLOW REYNOLDS NUMBER

FLOW REYNOLDS NUMBER

The model developed in the main body of this thesis was derived based on the assumption that the flow over the slide is ripple free laminar. A flow of the type on the slide will be ripple free if the Reynolds number is less and 4 to 25 (12). The flow Reynolds number, R_e, can be estimated as:

$$R_e = \frac{4\delta U_z(\text{ave})\rho_f}{\mu}$$

Substituting for δ and $U_z(\text{ave})$ from Equations (3) and (4) respectively into the above equation,

$$R_e = \frac{4\rho_f Q}{\mu}$$

It is necessary to substitute representative numerical values into the above equation to get the value of Reynolds number. A value of 0.01 centipoise is assumed for the viscosity term, μ. This represents the viscosity of water which is much lower than any oil analyzed using the Ferrogram. Normal flow rate through the peristaltic pump, Q, is of the order of 0.004 cubic centimetre per second. For a conserative approach assume Q as equal to 0.01 centimetres. Substituting these values into the equation for Reynolds number, the flow Reynolds number is equal to 3.2. Obviously, this value is much lower than the limit of Reynolds number equal to 4 to 25. The values for demonstration here used was highly conservative. Moreover, no ripples were ever observed on the fluid film during a large number of slides

prepared.

Hence, the flow over the slide can be accepted as ripple free laminar.

APPENDIX C

REPRESENTATIVE NUMERICAL VALUES

REPRESENTATIVE NUMERICAL VALUES

In order to demonstrate the influence of various parameters on the Ferrographic process, a set of representative numerical values are chosen. The values are given below:

Density of fluid, ρ_f = 0.8 gm/cc

Density of ferrous wear particles, ρ_p = 8 gm/cc

Acceleration due to gravity, g = 980 cm/sec^2

Inclination of slide with respect to vertical, β = 88.5°

Viscosity of sample fluid, μ = 20 centipoise.

Width of U-boundary, w = 0.45 cm.

Flow rate of fluid, Q = 0.9 cc/minute

To obtain the value of fluid film height, δ, substitute the above values into Equation (3). Accordingly,

Fluid film height, δ = 0.1 cm.

Volume susceptibility of ferrous particles, K of iron = 1000.

Product of field and field gradient in terms of magnetic force, H (dH/dx) = 125 dynes/cc.

VITA

Karunakaran S. Nair

Candidate for the Degree of

Master of Science

Thesis: THE PHYSICS OF ANALYTICAL FERROGRAPHY

Major Field: Mechanical Engineering

Biographical:

Personal Data: Born in Thakazhy, Kerala, India, May 2, 1948, the son of Mr. and Mrs. Sankara Pillai.

Education: Graduated from B. V. High School, Thakazhy, India, in March, 1964; received the Bachelor of Science degree in Mechanical Engineering from Kerala University, India, in May 1970; underwent one year training in Aeronautical Engineering in the Indian Institute of Science, Bangalore, India, in December, 1972; underwent one year training in Flight Control and Simulation in the Indian Institute of Science, Bangalore, India, in August, 1976; completed the requirements for the Master of Science degree at Oklahoma State University in December, 1980.

Professional Experience: Technical Assistant, Indian Space Research Organization, Trivandrum, India, 1971; Hydraulics and Control Systems Testing Engineer, Hindustan Aeronautics Limited, Bangalore, India, 1972-1978; Graduate Research Assistant, Fluid Power Research Center, Oklahoma State University, 1978-1980; Training in Ferrography Operators Course at Foxboro Analytical, Boston, Massachusetts, June, 1980.